No. 2525

R. Frauenfelder[a]*, Matt J. Lato[a,b], Marek Biskupič[c,d]
[a] Norwegian Geotechnical Institute, P.O. Box 3930 Ullevaal Stadion, 0806 Oslo, Norway – Regula.Frauenfelder@ngi.no
[a, now at b] BGC Engineering Inc., Ottawa ON, Canada – mlato@bgcengineering.ca
[c] Avalanche Prevention Center, Otupné 111, 032 51 Demänovská Dolina, Slovakia – avalanches@hzs.sk
[d] Institute for Environmental Studies, Charles University, Ovocný trh 3-5, 116 36 Praha 1, Czech Republic

Automatic detection of avalanche debris based on very high resolution earth observation data

We applied an object oriented mapping algorithm developed in eCognition in order to automatically identify and digitally map avalanche debris in very-high resolution optical earth observation data. The algorithm performance is compared with respect to a selected number of avalanche outlines in the High Tatra manually detected and mapped by avalanche experts. In addition, we explored the applicability of Sentinel-1 data for avalanche detection and mapping.

Pictures: Avalanches in the Žiarska valley and the area of the Belianske Tatry, photographs taken on April 1, 2009. Source: Slovakian Avalanche Prevention Center (APC).

Spring 2009 avalanche cycle

During the winter of 2008/2009 an large avalanche cycle occurred basically over the entire Slovakian mountain range. The cycle peaked in the period from 25th to 31st of March resulting in more than 200 avalanches in the area of the Tatra national park (738 km^2). The whole spectrum of avalanche sizes were observed, ranging from small ones to very large ones (some of which with return periods of up to 100 years). Several huts, bridges, two automatic weather stations and 1 km^2 of forest were destroyed.

Available data

The Slovakian Avalanche Prevention Center (APC) acquired WorldView-1 imagery from April 2, 2009, covering parts of the Tatra Mountains (Fig. 1) , in order to detect and map avalanches in regions that were inaccessible for the field teams.

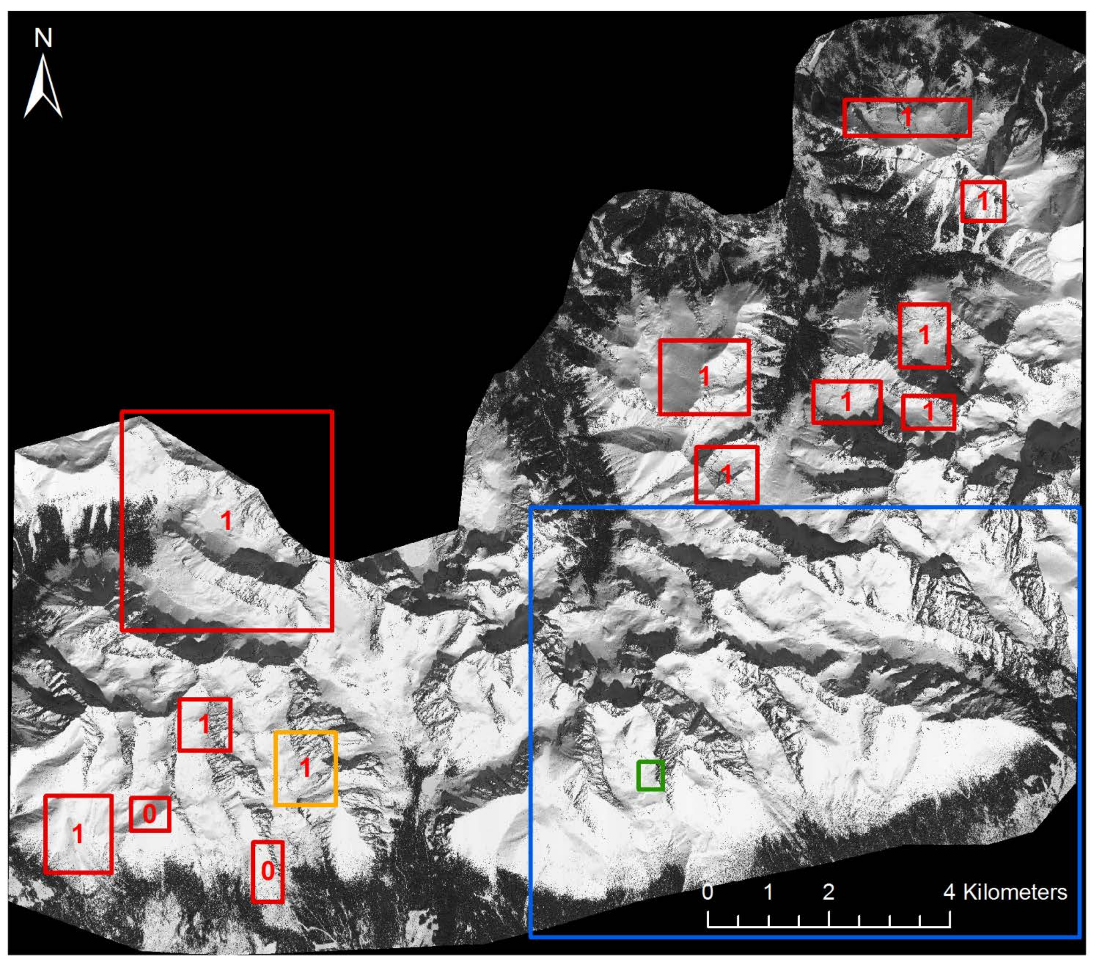

Figure 1: Study region: blue rectangle = algorithm training area; green rectangle = example shown in Figure 2; red rectangles = randomly selected test areas for validation (0 = without avalanches; 1= with avalanches); orange rectangle = example shown in Figure 3. (Satellite image: Copyright © DigitalGlobe/WorldView-1; courtesy of APC).

Algorithm training

The algorithm that we applied was originally designed to perform on data from a multi-band, 12-bit opto-electronic pushbroom scanner (ADS40-SH52) by Leica-Geosystems and on VHR optical imagery from the QuickBird satellite (cf. Lato et al., 2012). The algorithm was subsequently trained further on WorldView imagery from Norway (not discussed here) and using part of the Slovakian imagery (marked with a blue rectangle in Fig. 1 above). We observed a distinct "rake" pattern in many lower-lying areas of the imagery. These features were presumably caused by a rain-on-snow event. We had to adapt the algorithm in order to eliminate these features prior to the actual avalanche debris mapping (Fig. 2).

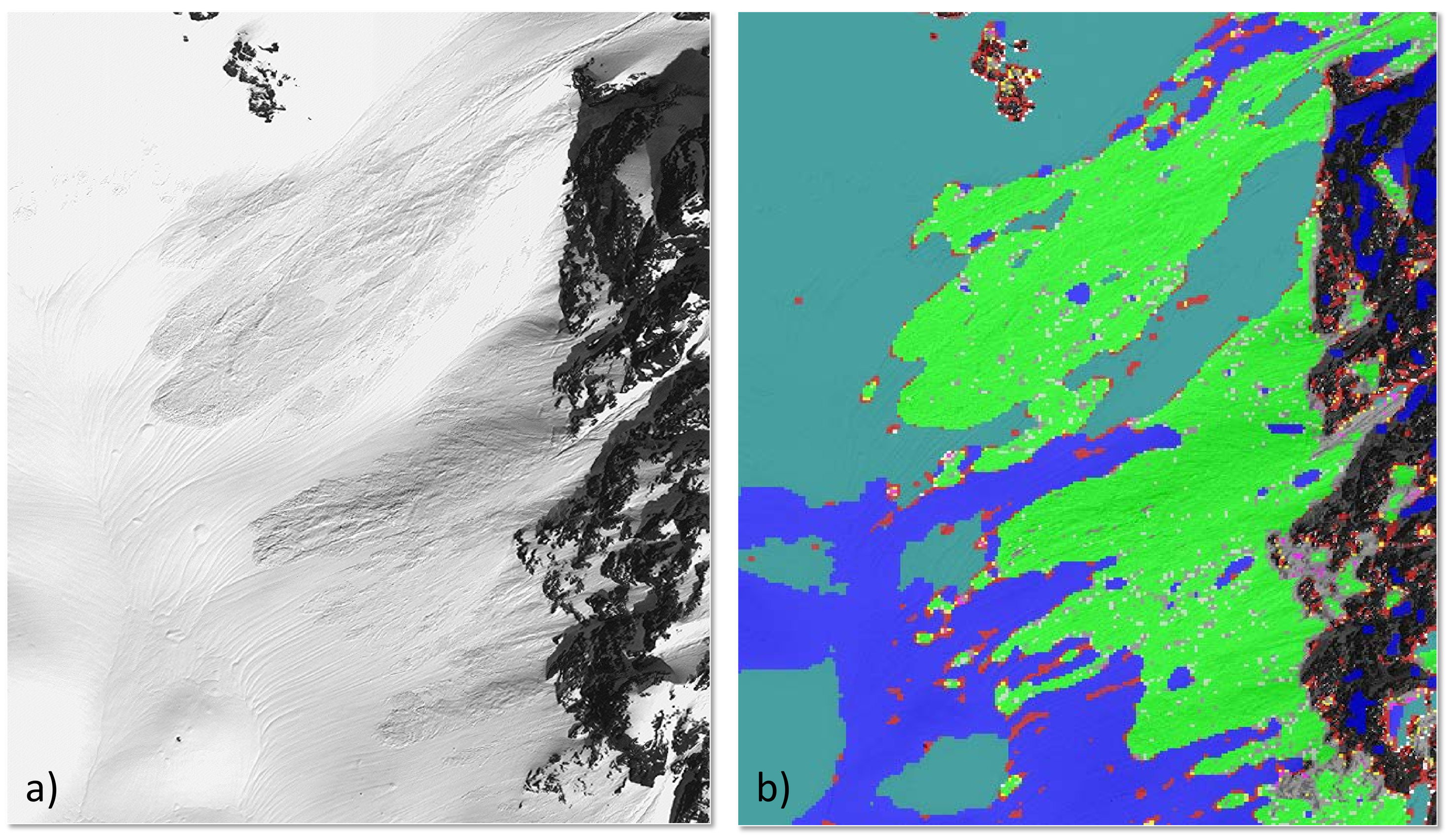

Figure 2: Classification result training stage (green rectangle in Fig. 1): a) raw image; b) automatic classification: green = avalanche debris; turquoise = glare and non-avalanche snow without rake pattern; blue = rake pattern; red = rock outcrops and forested areas. (Satellite image: Copyright © DigitalGlobe/WorldView-1).

Algorithm testing

The algorithm was tested and validated in randomly selected test areas of the Slovakian data set (red rectangles in Fig. 1). In order to quantitatively assess the performance of the algorithm, all avalanches in these test areas were visually identified and manually digitized by an avalanche expert. Fig. 3 illustrates the algorithm performance in one of the randomly selected test areas (marked in orange in Fig. 1).

Figure 3: Quantitative comparison (c) between expert mapping (a) and algorithm performance (b). Colour scheme in c) blue = mapped as avalanche snow by both; red = only mapped as avalanche by expert; yellow = only mapped as avalanche by algorithm. (Satellite image: Copyright © DG/WorldView-1).

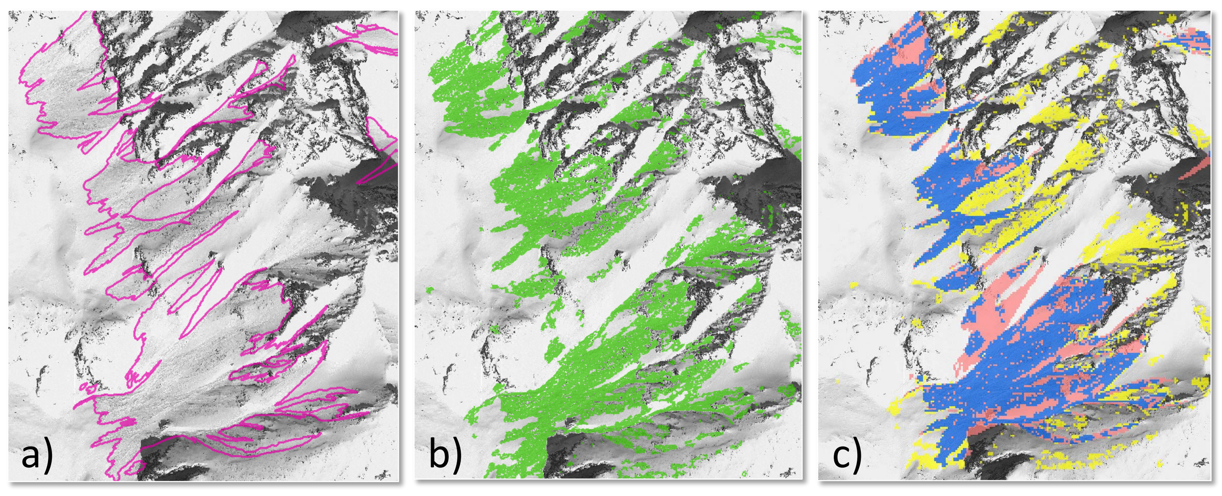

Figure 4 shows the algorithm results for the entire data set. The quantitative comparison (Table 1) of the automatic classification with respect to the expert mapping shows a good rate for the error of commission, however a considerably poor error of omission when considering the expert mapping as the "true" situation. The asymmetry of errors, or omission versus commission errors, is critical for the development of any image-classification algorithm. The main question hereby is if false positives (errors of commission) and false negatives (errors of omission) are equally negative to a mapping programme.

Table 1: Performance metrics of avalanche detection algorithm on Slovakian data set

Area error of commission (in %)	Area error of omission (in %)
22	59

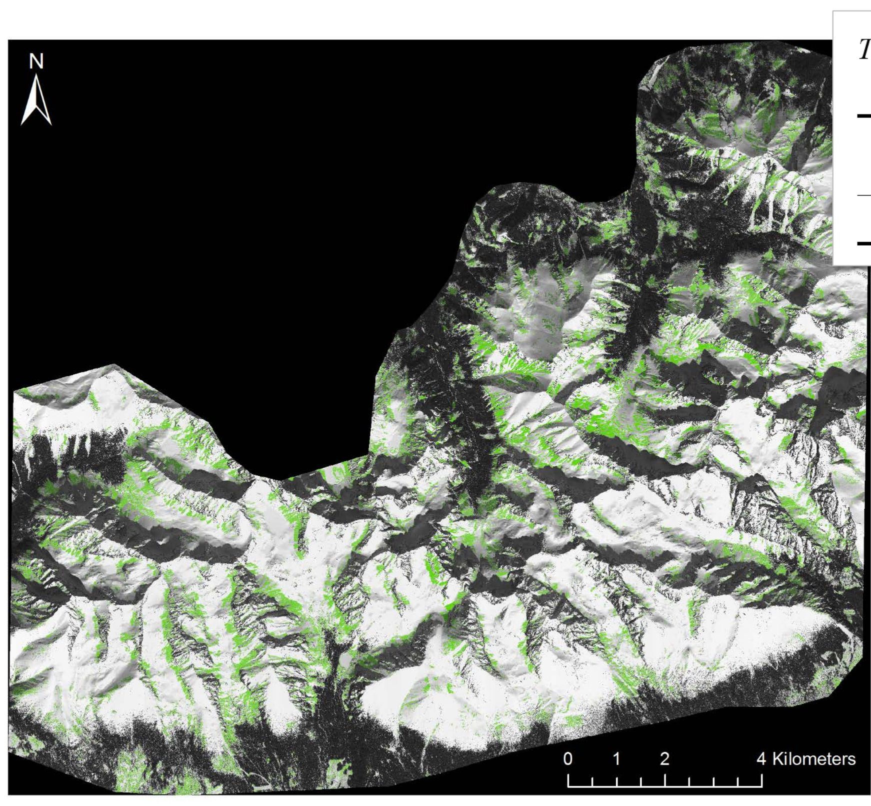

Figure 4: Automatic avalanche detection (in green) for the entire Slovakian study area. (Satellite image: Copyright © DigitalGlobe/WorldView-1; courtesy of APC).

Conclusions and outlook

We detect and map snow avalanche debris using an automatic detection algorithm implemented in eCognition. The method described and illustrated is flexible and easily adaptable to data from different very-high to high resolution optical sensors but needs further improvement before applicable in an operational setting.

A large drawback of optical methods is their dependency of clear sky conditions and good illumination. In order to be able detect avalanches also during bad weather conditions or during polar night, we test the feasibility to use SAR-data from the Sentinel-1 satellite for avalanche detection and mapping as shown by Malnes et al. (2015) and by Malnes in NGI (2015). An example from one of our study region is shown below (Fig. 5).

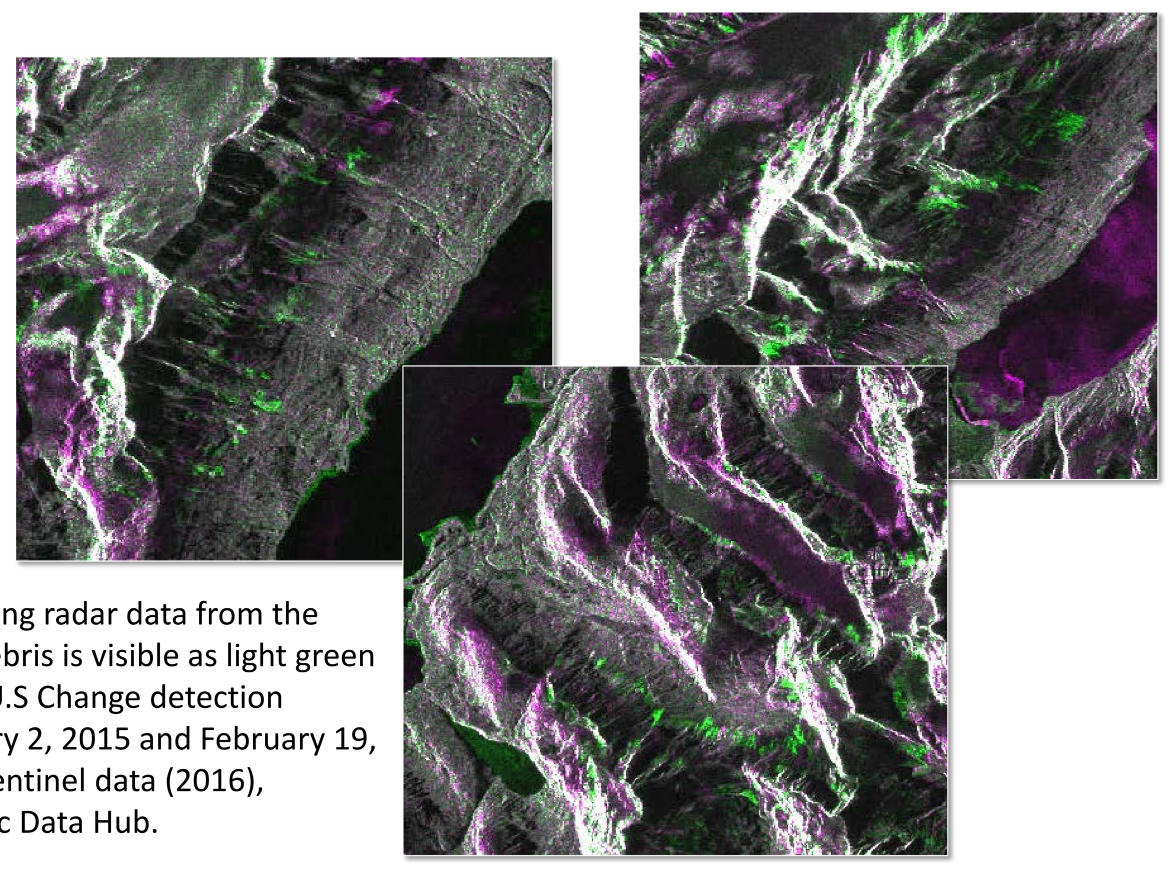

Figure 5: Avalanche detection using radar data from the Sentinel-1 satellite: Avalanche debris is visible as light green blotches. Example from Alaska, U.S Change detection between two scenes from January 2, 2015 and February 19, 2015. Data source: Copernicus Sentinel data (2016), retrieved from Sentinels Scientific Data Hub.

Further reading

- Lato, M., Frauenfelder, R., Bühler, Y. 2012. Automated detection of snow avalanche deposits: segmentation and classification of optical remote sensing imagery. Nat. Haz. And Earth. Syst. Sci., 12: 2893–2906
- Malnes, E., Eckerstorfer, M., Vickers, H. 2015. First Sentinel-1 detections of avalanche debris. The Cryosphere Discuss., 9: 1943–1963.
- NGI (2015): Towards an automated snow property and avalanche mapping system (ASAM) - Avalanche recognition and snow variable retrieval, version 2 (Technical report). NGI Report no. 20130092-04-R. 127 p.

Acknowledgements

This contribution was partly funded by the ESA PRODEX project ASAM ("Towards an automated snow property and avalanche mapping system"; contract no. 4000107724). Galina Ragulina (NGI) is acknowledged for her meticulous manual mapping of the numerous avalanches. Data sources: WorldView-1 from the Tatra Mountains was obtained with the support of the Slovakian Ministry of Interior, Depart. of Scientific and Technological Development; Sentinel-1 data: Copernicus Sentinel data (2015), retrieved from Sentinels Scientific Data Hub.

ON SAFE GROUND